

Demonstration of Inter-Vehicle UWB Ranging to Augment DGPS for Improved Relative Positioning

Mark G. Petovello, Kyle O'Keefe, Billy Chan, Stephanie Spiller, Cyril Pedrosa, Peng Xie¹, Chaminda Basnayake²

¹ Dept. of Geomatics Engineering, University of Calgary Schulich School of Engineering, 2500 University Dr. NW, Calgary, Alberta, Canada, T2N 1N4

² Electrical and Controls Integration (ECI) Laboratory, General Motors Technical Centre

Abstract

Vehicle-to-vehicle (V2V) navigation is reviewed and the concept of differential GPS relative navigation augmented with ultra-wideband (UWB) and bearing measurements is introduced theoretically. Filtering software is developed and tested using a data set collected between three moving vehicles in a test in Calgary. Initial results combining GPS pseudorange, UWB range and bearing measurements show that the additional measurements can significantly improve horizontal positioning accuracy, particularly in environments where GPS availability is poor. The UWB measurements generally contributed to an improved along-track relative position while the bearing measurements improved the across-track position. Whether or not the azimuth of the vehicle making the bearing measurement is known a priori or estimated by the filter is shown to have very little effect on the performance. Data from the three-vehicle test was also used to characterize UWB systematic errors in the V2V environment.¹

Keywords: GPS, Ultra-wideband, Vehicle-to-vehicle relative navigation

1. Introduction

Vehicle navigation has received considerable attention in the navigation community because of its importance in intelligent transportation systems. Many, if not all systems, are heavily reliant on GNSS data to compute vehicle positions and some systems also integrate other sensors such as accelerometers, gyroscopes and odometers to further improve results, especially when GNSS data is less available or unavailable altogether. In

many cases, these investigations have led to satisfactory position determination in a wide range of applications and operational environments.

However, several applications are not interested in solving absolute positioning problems such as "what road am I on?" Instead, many applications are concerned with determining relative position of nearby vehicles and/or infrastructure (e.g., intersections). In this case, the relevant question becomes "where is the nearest vehicle to my current position?" Vehicle-to-vehicle (V2V) and Vehicle-to-infrastructure (V2I) positioning are two of the key technologies for vehicle safety applications. However, to be effective, sub-metre to decimetre-level accuracy is required. As with absolute positioning, GNSS can also be applied here through operation in differential mode between vehicles. This approach has been used successfully in the past (e.g. Luo and Lachapelle 2003). However, to obtain the accuracy required for safety applications, either carrier-phase methods must be employed, or measurements from additional sensors must be added to improve the differential pseudorange GNSS solution.

The objective of this paper is to augment GNSS – specifically differential L1 GPS – for V2V relative positioning by using between-vehicle range and bearing measurements. The range measurements are obtained using ultra-wideband (UWB) radios.

UWB is a relatively new radio technology that allows for precise (cm- to dm-level) short distance (<300 m) ranging. UWB transmissions are usually defined as those with a fractional bandwidth (with respect to carrier frequency) greater than 0.20 or greater than 500 MHz (regardless of the fractional bandwidth). UWB signals have been used for radar, short-distance/high-rate communication, and ranging. UWB systems can broadly be categorized into impulse UWB (using nano-second long pulses with or without a carrier) or multi-carrier UWB (using orthogonal frequency-division multiplexing). In both cases, an extremely wide

¹ This paper is a revised and expanded version of a paper presented at the 2010 Institute of Navigation GNSS Meeting.

bandwidth signal is transmitted, resulting in very precise time-resolution and excellent multipath rejection capabilities. To minimize potential interference with narrowband communications systems, UWB signals are required to have extremely low powers, which results in limited operational ranges.

An additional advantage of UWB ranging is that several proposed ranging protocols also support data transfer. Although the automobile industry is currently developing dedicated short-range radio communication protocols for inter-vehicle communication (Kenney, 2011), UWB systems could also be used for V2V communication.

The UWB radios used in this work modulate a 6.35 GHz carrier with a 3 ns Gaussian-like pulse resulting in a signal with a bandwidth of approximately 500 MHz and a ranging precision of better than 15 cm (Fontana, 1999).

By combining the UWB range measurements with DGPS data, the relative positioning accuracy and reliability are both improved. Previous work by the authors (Petovello et al 2012) has included simulation (covariance) studies using pseudorange data combined with various other sensors for relative positioning. This paper expands on this work in three main ways.

First, data collected with three or more vehicles simultaneously is processed together to approximate the situation where a small cluster of vehicles are traveling together. By exchanging GPS and UWB data between the vehicles, a form of collaborative positioning is obtained that provides improved performance over GPS alone. Bearing observations have been generated using inertially aided reference trajectories of the vehicles and the benefit of adding these observations to the solution is explored.

Second, the effect of knowing or not knowing the azimuth of the vehicle making bearing measurements is assessed. Both cases provide nearly identical performance, meaning that additional sensors are not required by the vehicle to determine its azimuth.

Third, the UWB range errors during relative motion are thoroughly investigated. Previous studies (Cardinali et al 2006; MacGougan et al 2009) have only included static transceivers, which are not necessarily representative of kinematic performance.

The remainder of this paper is organized as follows. First, the two observation types – namely UWB and bearing – used to augment GNSS are introduced. Then an extended Kalman filter designed to estimate the relative locations of the group of moving vehicles using GPS, UWB and bearing observations is presented. The

filter is then tested using real data collected with three vehicles. Various combinations of measurement are used to determine the absolute and relative performance. Also, when integrating bearing observations, consideration is given to the case where the azimuth of the vehicle making the measurement is unknown. The UWB range measurements are then assessed to better determine their systematic errors.

2. Measurement Models

GPS pseudorange, Doppler, phase measurements, UWB ranges, and vehicle bearing measurements are combined in a relative navigation filter. GPS measurement models are well known and can be found in standard texts (e.g., Leick 2004; Kaplan et al 2006; Misra and Enge 2006).

2.1 UWB range model

The second measurement type used is the UWB range, P_{ab}^{UWB} , between radios a and b . The measurement model is given by

$$P_{ab}^{UWB} = \rho_{ab} + \varepsilon_{ab}^{UWB} \quad (1)$$

where ρ_{ab} is the geometric distance between the two radios and ε_{ab}^{UWB} are the UWB measurement errors. It is noted that there is no receiver clock error, since the UWB radios used employ a two-way ranging technique. Furthermore, the measurement errors are different than in the GPS case and include bias and scale factor errors, multipath and noise (MacGougan et al 2009). The bias and scale factor effects are initially ignored as they are on the order of code DGPS position errors, but they are then taken into account in order to obtain a UWB aided phase solution, as initially demonstrated in (MacGougan et al 2010), in the final section of the paper. Linearizing equation (1) gives

$$\Delta P_{ab}^{UWB} - \Delta \hat{\rho}_{ab}^{UWB} = H [\delta \Delta \vec{r}_{ab}] + \Delta \varepsilon_{ab}^{UWB} \quad (2)$$

where H is a row matrix containing direction cosines corresponding to the line of sight between the two UWB radio involved in the measurement.

2.2 Bearing model

Bearing is an angular measure of the horizontal direction of another vehicle relative to the *forward direction* of the vehicle making the measurement. The concept is shown graphically in Fig. 1, where β_{ab} is the bearing measurement from vehicle a to b . Also shown, are the azimuth of vehicle a , denoted α_a , and the azimuth of the relative position vector ($\Delta \vec{r}_{ab}$), denoted α_{ab} .

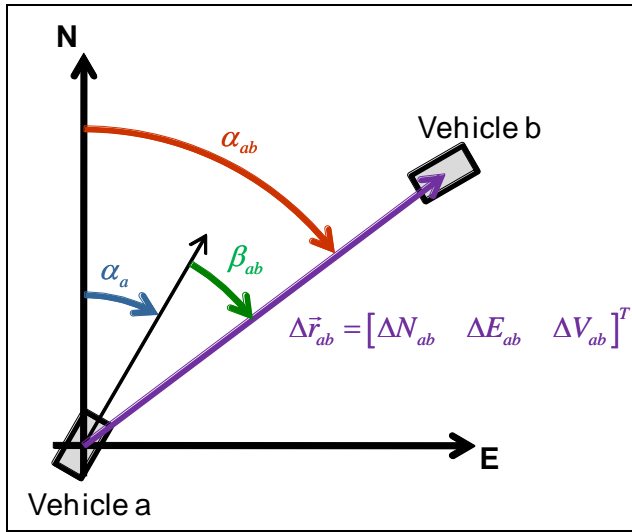


Figure 1: Graphical Representation of a Bearing Measurement

From Fig. 1, the bearing measurement can be written mathematically as

$$\beta_{ab} = \alpha_{ab} - \alpha_a. \quad (3)$$

However, the azimuth of the relative vector can be written as

$$\alpha_{a,b} = \tan^{-1} \left(\frac{\Delta E_{ab}}{\Delta N_{ab}} \right) \quad (4)$$

where ΔN_{ab} , ΔE_{ab} and ΔV_{ab} (shown in Fig. 1) are the north, east and vertical components of the relative vector. Substituting this result into equation (3) gives the final equation for the bearing measurement

$$\beta_{ab} = \tan^{-1} \left(\frac{\Delta E_{ab}}{\Delta N_{ab}} \right) - \alpha_a \quad (5)$$

Linearizing equation (5) and adding measurement noise, ε_{ab}^β , gives

$$\beta_{ab} - \hat{\beta}_{ab} = H_\beta [\delta \Delta \vec{r}_{ab}] - \delta \alpha_a + \varepsilon_{ab}^\beta \quad (6)$$

It is important to note that to use the bearing measurement one needs to know – or have an estimate of – the azimuth of the vehicle making the measurement. Specifically, this is needed to relate a bearing measurement, which is made in the frame of vehicle making the measurement, to a globally-referenced frame (in this case, the local level frame). In turn, this leads to two separate implementation options. In the first case, the azimuth of the vehicle making the bearing measurement is assumed to be known, for example, from another on-board navigation system or other sensors. In this case, the $\delta \alpha$ term in equation (6) is zero (i.e., no error in the estimated value). The second case assumes

the azimuth of the vehicle making the bearing measurement is unknown and must, therefore, be estimated along with the relative position states. The former case is preferred, since it removes one unknown for every bearing-measuring vehicle in the network. Both the azimuth-known and azimuth-unknown cases are considered here.

3. Integration Filter

This section describes the details for how the integrated system was developed. It begins with the concept of a “lead vehicle”, which is central to the relative positioning problem. The section concludes with a discussion of the various aspects of the estimation algorithms used.

3.1 Concept of a lead vehicle

From a positioning standpoint, the primary GPS measurements used are the between-receiver single difference pseudoranges. Using these measurements, the *absolute* position of the receivers cannot be determined. To account for this, we herein refer to a “lead vehicle” whose position is assumed known. The absolute positioning accuracy of the lead vehicle need not be very stringent. Specifically, with reference to Tang (1996) the effect of reference station (lead vehicle) position error on the baseline solution is closely approximated by

$$\|\delta \Delta \vec{r}\| \approx \frac{10^{-9} \|\delta \vec{r}_{base}\|}{\|\Delta \vec{r}\|} \quad (7)$$

where $\Delta \vec{r}_{base}$ is the error in base station position and $\Delta \vec{r}$ is the baseline vector. For the application at hand, assuming the lead vehicle has an absolute positioning error of 3 km the resulting error on the (maximum) inter-vehicle distance of 300 m will be on the order of 10^{-8} m, which is negligible. It is assumed that the position of the lead vehicle can be determined to this level of accuracy using standalone GPS data and/or other data that may be available.

With this in mind, the following sections provide more detail for computing the relative position and velocity of two receivers using Kalman filter estimation.

3.2 Estimation algorithm

The relative navigation solution is implemented using an extended Kalman filter where between receiver single difference GPS pseudorange and Doppler observations are used. In cases where the two other vehicles observe a GPS satellite that is not visible to the lead vehicle, the option exists to add this single difference as well. UWB and bearing observations are also included both individually and together.

The elements of the state vector vary according to what type of processing is being done. Relative position, clock bias, velocity and clock drift states are included for each non-lead vehicle in the network and, as stated previously, are all relative to the lead vehicle. Azimuth states are included only for bearing-measuring vehicles and only when the azimuth is assumed to be unknown.

The relative velocities are modeled as a first order Gauss-Markov processes with a 2 second time constant. The horizontal standard deviation is 10 m/s and the vertical standard deviation is 1 m/s. These values were obtained by analyzing the reference solution velocities from a field data collection discussed below.

The receiver clock drift is modeled as a first order Gauss-Markov process with a 1000 m/s standard deviation and 10 second time constant. The assumed accuracies of the three measurement types are given in Table 1.

Table 1: Summary of Measurement Accuracy

Measurement	Standard Deviation
Undifferenced GPS Pseudorange	5 m
UWB Range	0.5 m
Bearing Measurement	0.5°

3.3 Covariance analysis

A detailed covariance analysis of the above GPS, UWB and bearing integration was conducted for a number of simulated urban canyon environments, varying numbers of vehicles, and varying measurement qualities (Petovello et al 2012). The results are not reported here, however the main findings demonstrate that the addition of UWB observations generally improves the estimated accuracy in the along-track component of the relative positions, while the addition of bearing observations improves the across-track component. This is a result of the simulated geometry of the groups of vehicles, where all the vehicles were traveling in the same direction in up to three different lanes on the same road. A second main finding was that in the case of three or more vehicles making both UWB and bearing observations, these two measurements alone are sufficient to completely determine the relative horizontal navigation solution. As a result, the accuracy and reliability in this situation is mainly a function of the UWB and bearing measurement accuracies, which are generally better than those of code DGPS observations. The results obtained from real data, presented in the next section, support these findings.

4. Three-Vehicle Data Collection

To demonstrate the algorithm presented above under operational conditions and to assess the usefulness of UWB and bearing observations, a three vehicle field test was conducted on February 26, 2010 for approximately one hour. The test was performed around the University of Calgary and included areas of open sky, foliage and some obstructions due to buildings.

Each vehicle was equipped with a NovAtel OEMV3 GPS/GLONASS receiver, a NovAtel OEM4-DL GPS receiver and a Multi-Spectral Systems UWB radio (including necessary data logging computers). In addition, two of the vehicles were equipped with NovAtel SPAN systems, which provide GPS and time-tagged inertial measurement unit (IMU) data. A fourth NovAtel OEMV3 GPS/GLONASS receiver was placed on the roof of the CCIT building on the University of Calgary campus to serve as a base station for generating a reference solution. Table 2 summarizes the data collected and the purpose of each data source. Note that since a sensor for observing the bearing was not available, the bearing measurements used were generated from the reference solution after the fact, as described in more detail below.

Table 2: Summary of Data Collected

Equipment	Data Rate	Purpose
NovAtel OEMV3 GPS/GLONASS Receivers	20 Hz	Generation of reference solution only, which is also used to generate bearing measurements
NovAtel OEM4-DL GPS Receivers	20 Hz	Time tagging UWB data and data processing (with and without UWB and bearing measurements)
SPAN System (IMUs)	100 Hz	Improve reference solution and determine azimuth of vehicles in order to compute bearing measurements
MSS UWB Radios	3 Hz (average)	UWB measurements for processing

The equipment setup consisted of a NovAtel GPS-702GG antenna connected to the GNSS receivers in each of the three vehicles as well as the base station. A picture

of the equipment setup on one of the test vehicles can be seen in Fig. 2.



Figure 2: GPS, UWB and IMU Equipment Setup on a Test Vehicle

The UWB measurements were time tagged using the CPU time on the data collection computer. Range measurements from the UWB radios were transferred via a serial cable to the logging computer using the UWB data logging software. In order to ensure that the UWB observations were synchronized with GPS time, a software utility was used at the beginning of the data collection session to obtain the GPS time from the NovAtel OEM4-DL GPS receiver. This worked by obtaining the NMEA data stream sent from the OEM4-DL receiver via a serial port connection.

Approximately midway through the test, the UWB radio on the lead vehicle failed and had to be replaced with a backup unit. Consequently, the data processing is divided into two sections; one prior and one after switching the units. Finally, in this paper the vehicles are identified as the “lead vehicle”, “vehicle 1” and “vehicle 2”; the latter two being the non-lead vehicles.

4.1 Environment and Satellite Geometry

A map of the test route chosen is shown in Fig. 3 and can be roughly divided into three different sections. Open sky sections occur primarily along Shaganappi Trail and around the University (start/end point). Foliage is encountered in the residential area. Finally, partial urban canyons occur around the Alberta Children’s and Foothills hospitals. A view of the residential environment from one of the vehicles is shown in Fig. 4 while the view approaching the Alberta Children’s Hospital is shown in Fig. 5. Corresponding with the different environments, the number of visible satellites varied throughout the test. Fig. 6 shows the number of visible satellites from the lead vehicle. Furthermore, Fig. 7 shows the skyplot of visible satellites at the start and end of the test.

Finally, to get an idea for the relative motion of the vehicles, Fig. 8 shows the separation and bearing of the two non-lead vehicles relative to the lead vehicle. The UWB radio failure mentioned above occurred at approximately GPS time 502100 (1100 on the plot). It is identified by approximately 250 seconds of fixed separation and bearing while the three vehicles were stopped and the UWB radio was replaced with the spare.

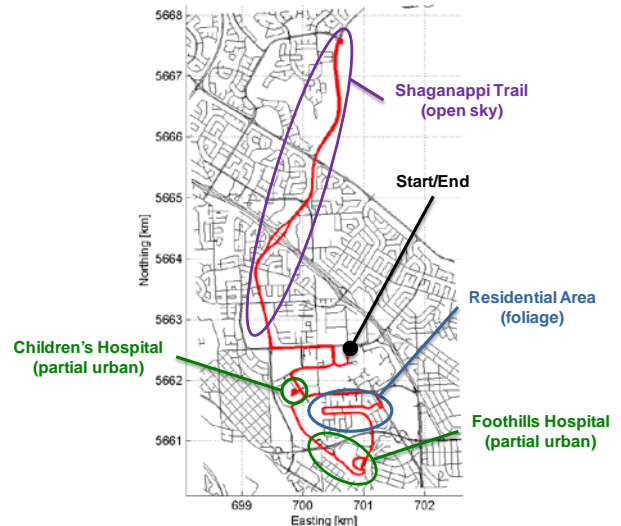


Figure 3: Field Test Route



Figure 4: View from Trailing Vehicle of the Other Two Vehicles in the Residential Area



Figure 5: View Approaching Alberta Children’s Hospital.

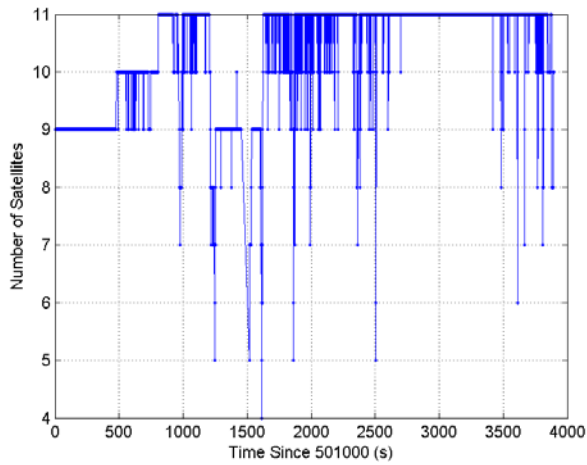


Figure 6: Number of Visible Satellites Measured by the Lead Vehicle

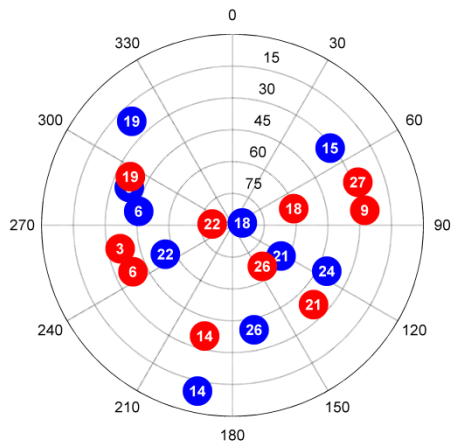


Figure 7: Skyplot of Visible Satellites at the Start (blue) and End (red) of the Field Test

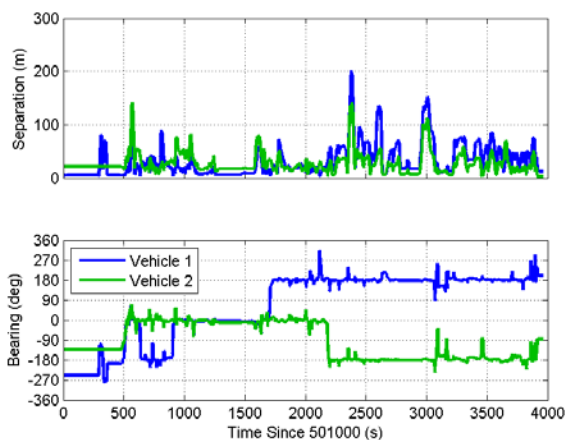


Figure 8: Separation and Bearing for Non-Lead Vehicles Relative to the Lead Vehicle Computed from the Reference Solution

4.2 Reference Solution

A reference trajectory for each of the three vehicles was generated by processing the GPS and GLONASS carrier observations – and IMU data, if available – using Waypoint’s Inertial Explorer and GrafNav software packages. A kinematic Ionosphere Free (IF) fixed ambiguity solution was specified and all solutions were computed relative to the base station on the University of Calgary campus. The estimated accuracy of each solution is better than 10 cm in each coordinate direction. The relative position of the different vehicles was then computed in the local level frame by inverting the reference positions. The accuracy of the relative position is similar to that of the individual positions (although noise should increase, the position errors between receivers will nevertheless be correlated).

4.3 Generation of Bearing Measurements

Since a bearing sensor was not available for this test, bearing measurements were generated from the reference trajectories and then used as input to the data processing software. Specifically, the first term in equation (5) is evaluated from the reference-derive relative positions and the second term is obtained from the processing of the IMU data. In this way, the bearing measurements are “perfect” to within the relative positioning accuracy over the vehicle separation. As a quick assessment, if the relative horizontal positioning accuracy is 10 cm per direction, or 14 cm horizontally, and the vehicles are separated by 28 m (i.e., the “two second” rule at 50 km/h), then the computed bearing is conservatively accurate to about 0.3 degrees ($= 0.14 \text{ m} / 28 \text{ m} \times 180 / \pi$).

4.4 Processing Software and Parameters

All of the algorithms discussed above were implemented in a C++ data processing program. The program is a modified version of a single-baseline static base station processing software previously developed (MacGougan et al 2010) with the addition of the ability to process multiple baselines including additional independent GPS observations between two baselines as well as bearing data.

The bearing measurements were assumed to have an accuracy of 0.5° (1σ). The UWB measurement blunders were manually removed from the data and UWB measurements were *not* corrected for bias or scale factor errors. Finally the azimuth state for each bearing observing vehicle was obtained from the inertially-aided reference trajectory and was not otherwise estimated in the filter.

5. Results

The effect of adding UWB and bearing observations is assessed in this section by comparing four different

combinations, namely GPS alone, GPS+UWB, GPS+Bearing, and GPS+UWB+Bearing.

To save space, results from the entire data set are not shown and instead several interesting subsections of the data are presented in detail below. With the addition of UWB ranges, the along-track components of the relative errors improve while the bearing observations improve the across-track. This is consistent with the covariance analysis mentioned previously and is expected since the vehicle configuration for the majority of the test involved the three vehicles traveling in a line separated at most in the across-track direction by about 3 metres (or one lane). Similarly, inclusion of the bearing measurements improves the across-track accuracy.

5.1 Partial Urban Canyon results

Of particular interest is a short segment of the test where the three vehicles drove west towards the Children’s hospital and then turned 180° in a traffic “loop” before exiting back to the main road. In the process, one satellite is lost from view as it becomes obstructed by the building. In addition, it is expected that the building would also act as a reflector to signals to the east, thus inducing multipath errors.

Fig. 9 and Fig. 10 respectively show the positioning errors for vehicle 1 and 2 in both the along and across-track directions. A few points are worth noting in these results. First, the GPS-only solutions are very good, with errors on the order of 10-20 cm. However, when adding UWB data, the solution is not improved. This is likely due to a combination of timing errors and the fact that the UWB measurements suffer from systematic errors that have neither been estimated nor compensated in this case (since the GPS-only solution is already has the same order of accuracy as the UWB measurements, the proper handling of the systematic errors is now critical). Poor time synchronization has the largest effect when relative vehicle dynamics are large. The addition of bearing data however results in significant improvement, especially in the across track direction.

Second, the systematic behaviors near 710 seconds and 740 seconds correspond to the vehicles turning into and then around in front of the hospital. As this happens, the errors shift between the along and across-track directions (which are defined in the frame of the lead vehicle). This should be obvious from the reference bearings to each of the vehicles, as shown in Fig. 11 (same as the lower plot in Fig. 8 but adjusted to the proper time scale). Specifically, the bearing measurements change by approximately 50 degrees for a few seconds and then 90 degrees 30 seconds later. During these periods, the UWB is effectively measuring the *across-track* range and the bearing measurement is constraining the *along-track* direction. Correspondingly, the benefits of each

sensor are effectively reversed from the typical case when vehicles follow each other down the road. This is perhaps most obvious for the bearing measurement.

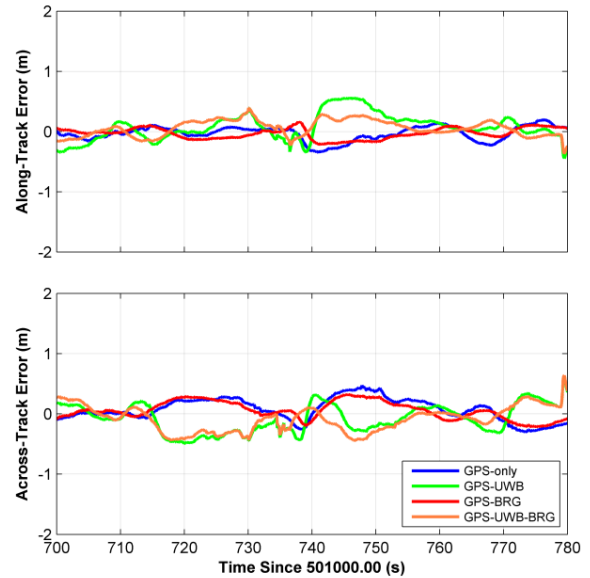


Figure 9: Along and Across-Track Errors for Vehicle 1 near Children’s Hospital

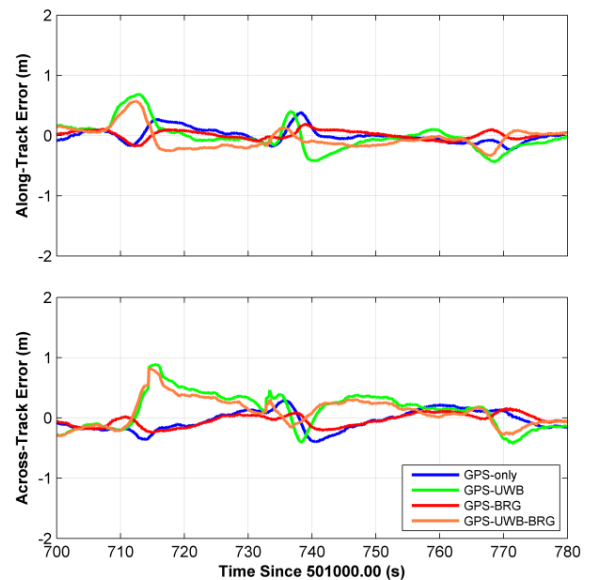


Figure 10: Along and Across-Track Errors for Vehicle 2 near Children’s Hospital

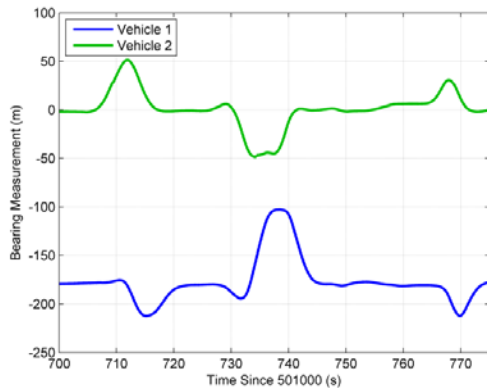


Figure 11: Bearing of Two Vehicles with respect to the Lead Vehicle in Front of Alberta Children’s Hospital

The statistics for the above results are summarized in Table 3 and Table 4. Overall, the values support the analysis of the figures.

Table 3: Along and Across-Track Error Statistics for Vehicle 1 in Front of Children’s Hospital

Solution	Along (m)		Across (m)	
	Mean	Std Dev	Mean	Std Dev
GPS-Only	-0.03	0.12	0.07	0.19
GPS+UWB	0.07	0.22	-0.08	0.23
GPS+Bearing	-0.03	0.09	0.06	0.15
GPS+UWB+Bearing	0.06	0.14	-0.09	0.21

Table 4: Along and Across-Track Error Statistics for Vehicle 2 in Front of Children’s Hospital

Solution	Along-Track		Across-Track	
	Mean	Std Dev	Mean	Std Dev
GPS-Only	0.00	0.12	-0.05	0.17
GPS+UWB	-0.01	0.23	0.13	0.29
GPS+Bearing	0.01	0.07	-0.04	0.10
GPS+UWB+Bearing	-0.05	0.17	0.10	0.23

5.2 Residential Areas

The next portion of data analyzed is from a residential area with significant foliage (e.g., see Fig. 4). Along and across-track errors are shown in Fig. 12 and Fig. 13 for vehicles 1 and 2 respectively. As can be seen, there is a short data outage starting around GPS time 502860 (1860 on the plots) followed by metre-level GPS errors.

The solutions involving UWB and/or bearing data are also affected. However, the key finding in this case is that by adding the other sensors, the errors are not only smaller but the solution converges much more rapidly to the correct solution. The most extreme example of this is the across-track error for vehicle 2 (lower plot in Fig. 12) which shows the GPS-only solution having an 80 cm bias after 40 seconds while the GPS+UWB solution has smaller bias and the bearing-aided solution returns to the correct value, with cm-level error immediately when GPS is reacquired. Table 5 and Table 6 summarize the error statistics for the two vehicles during this period of the test.

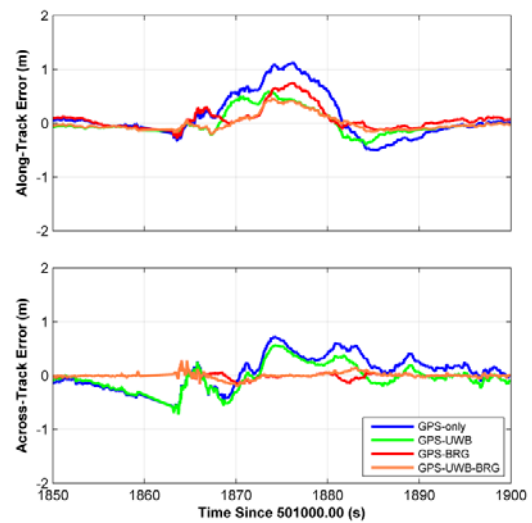


Figure 12: Along and Across-Track Errors for Vehicle 1 in Residential Area

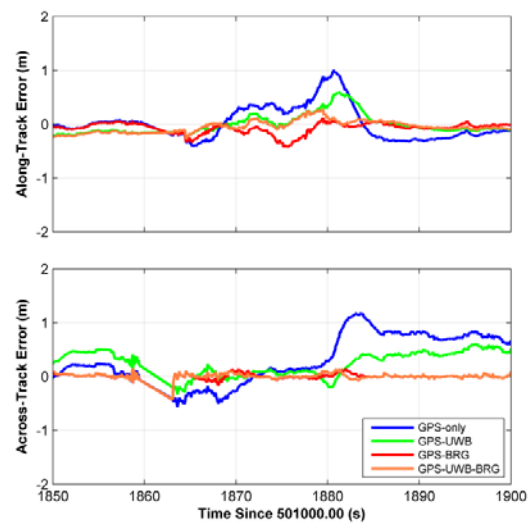


Figure 13: Along and Across-Track Errors for Vehicle 2 in Residential Area

Table 5: Along and Across-Track Error Statistics for Vehicle 1 Residential Area

Solution	Along (m)		Across (m)	
	Mean	Std Dev	Mean	Std Dev
GPS-Only	0.14	0.43	0.09	0.29
GPS+UWB	0.01	0.23	-0.01	0.24
GPS+Bearing	0.10	0.22	-0.01	0.05
GPS+UWB+Bearing	0.01	0.16	0.00	0.06

Table 6: Along and Across-Track Error Statistics for Vehicle 2 for Residential Area

Solution	Along (m)		Across (m)	
	Mean	Std Dev	Mean	Std Dev
GPS-Only	0.02	0.32	0.34	0.45
GPS+UWB	0.00	0.19	0.25	0.22
GPS+Bearing	-0.07	0.10	0.01	0.05
GPS+UWB+Bearing	-0.04	0.11	0.01	0.04

5.3 Estimation of Lead-Vehicle Azimuth

In the results presented previously assume that the lead vehicle (i.e., the vehicle making the bearing observations) has a known azimuth. Knowledge of this azimuth is required in order to integrate the bearing measurements with the differential GPS baselines being estimated. However, this may not always be true, in which case the azimuth of the vehicle would need to be estimated. The azimuth of the lead vehicle was therefore added as a state to the Kalman filter and the data set was reprocessed. The resulting errors in the estimated azimuth are shown in Fig. 14 for the first half of the data set, along with the azimuth rate obtained from the reference solution.

The estimated azimuth error is typically less than 0.2° with larger errors occurring during rapid vehicle manoeuvres. Similar results were obtained during the second half of the test. Given the ability to accurately estimate the vehicle azimuth, it is expected that the relative positioning errors with the azimuth unknown case should be similar to those in the azimuth known case.

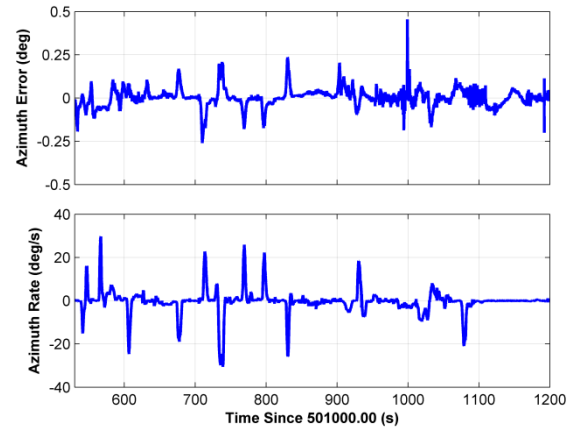


Figure 14: Lead Vehicle Azimuth Error and Azimuth Rate during the First Half of the Test

With this in mind, Fig. 15 shows the *difference* in the along and across-track position errors between the cases where the vehicle azimuth is known and unknown for vehicle 1. Note that only the GPS+BRG and GPS+UWB+BRG results are shown. As can be seen, the differences are typically at the centimetre level, especially for the GPS+UWB+BRG case. Furthermore, the larger errors correlate well with vehicle dynamics (see Fig. 14). Since these results are typical of both vehicles and for both halves of the test, results for vehicle 2 are not shown. Instead, the positioning error statistics are summarized in Table 7 for vehicle 1 and Table 8 for vehicle 2. Indeed, the statistics for the azimuth known and unknown cases are nearly identical.

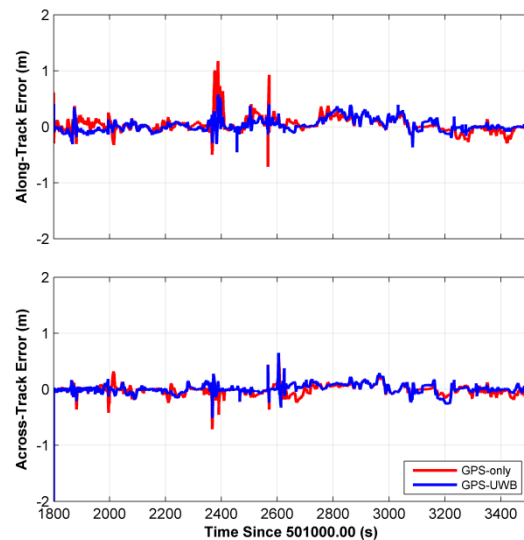


Figure 15: Along-Track and Across-Track Error Differences between the Azimuth Known and Unknown Cases for the First Half of the Test

Table 7: Along and Across-Track Error Statistics for Vehicle 1 with Azimuth Known and Unknown for First Section of the Test

Solution	Along (m)		Across (m)	
	Mean	Std Dev	Mean	Std Dev
GPS+Bearing	-0.02	0.13	0.00	0.14
GPS+Bearing Azimuth Unknown	-0.04	0.15	0.00	0.15
GPS+UWB+Bearing	0.00	0.16	0.00	0.19
GPS+UWB+Bearing Azimuth Unknown	0.00	0.18	0.00	0.19

The above results suggest that a bearing measurement is still useful even if the vehicle’s azimuth is unknown and needs to be estimated. Again, however, it must be borne in mind that since the bearing measurements used in this case are effectively perfect, the results are optimistic. Furthermore it should be noted that in this case two bearing measurements were available at all times, meaning one of them can effectively be used to estimate the vehicle azimuth while the other contributes to the position solution. If the bearing measurements were intermittent or only available one at a time, then the usefulness of the measurements would depend more on the quality of the lead vehicle azimuth estimate.

Table 8: Along and Across-Track Error Statistics for Vehicle 2 with Azimuth Known and Unknown for First Section of the Test

Solution	Along (m)		Across (m)	
	Mean	Std Dev	Mean	Std Dev
GPS+Bearing	0.16	0.60	0.04	0.48
GPS+Bearing Azimuth Unknown	0.06	0.53	0.05	0.42
GPS+UWB+Bearing	0.06	0.29	0.02	0.21
GPS+UWB+Bearing Azimuth Unknown	0.02	0.24	0.00	0.17

5.4 UWB Errors during Relative Motion

The inclusion of GPS phase measurements is only really useful if the phase ambiguities can be resolved. In the results presented in the previous section, the ultra-wideband measurements were used “as recorded” by the UWB ranging radios (less blunders). In previous studies involving stationary UWB radios, it was determined that the UWB radios suffer from systematic errors (bias and scale factor). As the eventual goal is a GPS phase

solution, for UWB to provide any benefit for ambiguity resolution, it will be necessary to improve the accuracy of the UWB measurements from the approximately 50 cm level used in previous sections to an accuracy of less than 10 cm. The UWB radios are theoretically capable of cm level observation accuracy, however only if the systematic effects can be controlled.

To assess the UWB systematic errors under kinematic conditions, the measured UWB errors were compared to the inter-vehicle baselines computed using the reference trajectory. UWB range errors are plotted as a function of range in Fig. 16. For ranges below 80 m, there is a large data set and an approximately linear trend, supporting the earlier results and theoretical expectations that the UWB measurements suffer, at least to first order, from bias and scale factor errors that change from run to run. Range error was also plotted as a function of relative velocity but this showed no systematic effects.

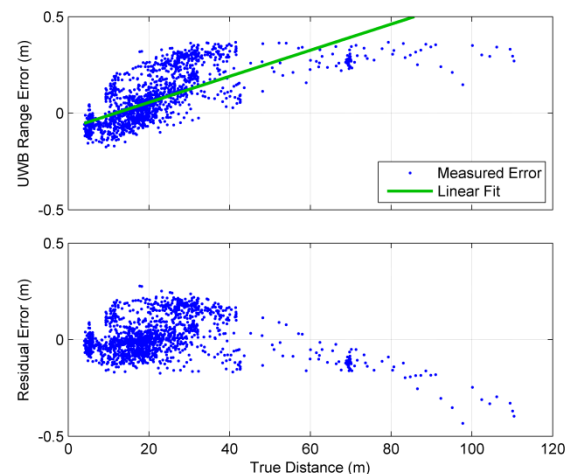


Figure 16: UWB Range Error as a Function of Reference Solution Distance for Lead Vehicle to Vehicle 1

Work to develop a better model for the systematic effects is ongoing. One hypothesis is that the error is dependent on the received signal strength, which is, in theory, proportional to the square of the range. To test this, in Fig. 17 the range error plotted versus distance squared on log scale, which exhibits a closer linear fit over a wider range of the observations than does Fig. 16. This is an area of ongoing investigation.

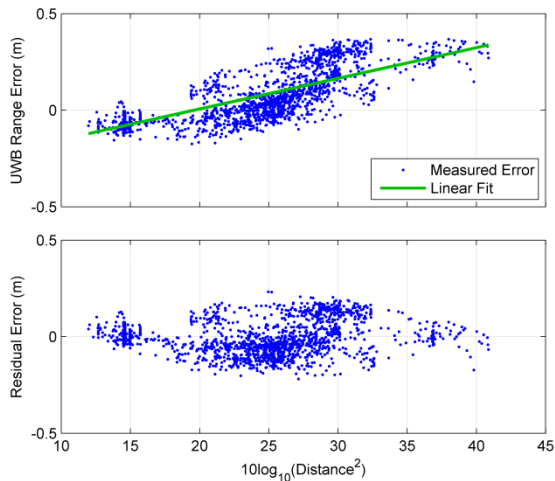


Figure 17: UWB Range Error as a Function of $10\log_{10}(\text{Distance}^2)$ for Lead Vehicle to Vehicle 1

6. Conclusions and future work

This paper investigated the performance of a relative positioning filter using different combinations of sensors in a real-world environment. The UWB range observations were found to provide the most benefit in the along-track direction and the bearing data providing the most benefit in the across-track direction.

However the usefulness of UWB measurements was limited by systematic errors in the data. To develop an operational system additional investigation is required to develop an improved model for these systematic effects, and/or to implement a method to estimate the systematic effects along with the relative navigation solution.

Acknowledgements

The research presented in this paper was conducted as part of a collaborative research and development grant between the University of Calgary, General Motors of Canada, and Natural Sciences and Engineering Research Council of Canada. Additional funding was also provided by Alberta Innovates Technology Futures (formerly Alberta Ingenuity Fund).

References

Cardinali, R., L. D. Nardis, M.-G. D. Benedetto & P. Lombardo (2006), *UWB Ranging Accuracy in High- and Low-Data-Rate Applications*, IEEE Transactions on Microwave Theory and Techniques Vol. 54, No. 4, pp 1865-1875.

Fontana, R. J. (1999), *Ultra wideband receiver with high speed noise and interference tracking threshold*, US Patent 005901172.

Kaplan, E. D., J. L. Leva, D. Milbert & M. S. Pavloff (2006), *Fundamentals of Satellite Navigation in Understanding GPS Principles and Applications*, E. D. Kaplan and C. J. Hegarty, eds., Artech House, Inc., Boston.

Kenney (2011), Dedicated Short-Range Communications (DSRC) Standards in the United States, *Proceedings of the IEEE*, Vol 99, No. 7, pp 1162-1182.

Leick (2004), *GPS Satellite Surveying*, John Wiley and Sons, Hoboken, NJ.

Luo, N. and G. Lachapelle (2003), *Relative Positioning of Multiple Moving Platforms using GPS*, IEEE Transactions on Aerospace and Electronic Systems, Vol 39, No.3, pp. 936-948.

MacGougan, G., K. O'Keefe & R. Klukas (2009), *UWB ranging and ranging measurement accuracy*. Measurement Science and Technology, Vol. 20, No. 9, Article No. 095105, 13 pages, doi:10.1088/0957-0233/20/9/095105.

MacGougan, G., K. O'Keefe & R. Klukas (2010), *Tightly-coupled GPS/UWB Integration*, Journal of Navigation, Vol. 63, No. 1 pp. 1-22. doi: 10.1017/S0373463309990257.

Misra, P. and P. Enge (2006), *Global Positioning System Signals, Measurement, and Performance*, Ganga-Jamuna Press, Lincoln, MA.

Petovello, M., K. O'Keefe and P. Wei (2012), *Assessment of Different Sensor Configurations for Collaborative Driving in Urban Environments*. International Journal of Observation and Navigation, in press.

Tang, C. (1996), *Accuracy and Reliability of Various DGPS Approaches*, M.Sc. Thesis, Geomatics Engineering, University of Calgary, Calgary

Biography

Mark Petovello is an Associate Professor in the Position, Location And Navigation (PLAN) group in the Department of Geomatics Engineering at the University of Calgary. Since 1998, he has been involved in various navigation research areas including software receiver development, satellite-based navigation, inertial navigation, reliability analysis and dead-reckoning sensor integration. His email is: mark.petovello@ucalgary.ca.